Angewandte
International Edition Chemie

Photocatalysis

International Edition: DOI: 10.1002/anie.201504933
German Edition: DOI: 10.1002/ange.201504933

Conversion of Carbon Dioxide by Methane Reforming under Visible-Light Irradiation: Surface-Plasmon-Mediated Nonpolar Molecule Activation

*Huimin Liu, Xianguang Meng, Thang Duy Dao, Huabin Zhang, Peng Li, Kun Chang, Tao Wang, Mu Li, Tadaaki Nagao, and Jinhua Ye**

Abstract: *A novel CO_2 photoreduction method, CO_2 conversion through methane reforming into syngas (DRM) was adopted as an efficient approach to not only reduce the environmental concentration of the greenhouse gas CO_2 but also realize the net energy storage from solar energy to chemical energy. For the first time it is reported that gold, which was generally regarded to be inactive in improving the performance of a catalyst in DRM under thermal conditions, enhanced the catalytic performance of Rh/SBA-15 in DRM under visible-light irradiation (1.7 times, CO_2 conversion increased from 2100 to 3600 $\mu mol\,g^{-1}\,s^{-1}$). UV/Vis spectra and electromagnetic field simulation results revealed that the highly energetic electrons excited by local surface plasmon resonances of Au facilitated the polarization and activation of CO_2 and CH_4 with thermal assistance. This work provides a new route for CO_2 photoreduction and offers a distinctive method to photocatalytically activate nonpolar molecules.*

Converting CO_2 into high-value-added chemicals offers a promising and challenging route for the environmental targets on reducing CO_2 emission.[1] Simultaneously, storing the abundant solar energy into renewable fuels provides a convenient mode to relieve the energy crisis caused by the increasing fossil fuels consumption.[2] The ideal vision is to convert CO_2 photocatalytically with H_2O, nevertheless, there is a long way to go because of the sluggish nature of CO_2 and H_2O in activation. Current studies were mainly focused on the photoreduction of CO_2 into CO or CH_4 by employing H_2 as the reductant,[3] which could reduce the environmental concentration of CO_2 whereas the downhill reactions are not favorable for energy storage. Dry reforming of methane (DRM), converting two kinds of greenhouse gases CO_2 and CH_4 into syngas (CO and H_2), is an uphill reaction and beneficial for the sustainable development of energy stratagem.[4] It has been extensively studied in thermal catalysis,[4,5] however, there were no reports on the reaction driven by solar energy up to now.

For DRM reaction, the high reaction barrier associated with the successive activation of CH_4 and CO_2, requires it to be operated at high temperatures (800–1000 °C).[6] It is known that, without the help of special apparatus, the temperature induced by solar light is usually very low, and even on the group-VIII-metal-based catalysts, the highest temperature was about 400 °C with the irradiation of 300 W Xe arc lamp,[3a] which is not high enough to initiate the DRM reaction.[6] Therefore, herein both photon energy (visible light) and thermal energy were employed as the energy input to meet the temperature requirement of DRM.

As for CO_2, it is difficult to be photocatalytically one-electron activated because of its −1.9 eV reduction potential,[7] which is above nearly all the conduction band of the known semiconductors. Earlier reports disclosed that, compared with the traditional thermal method, CO_2 could be more easily activated by plasma by collision with the highly energetic plasma electrons.[8] Gold (Au) was reported to have the property of local surface plasmon resonances (LSPRs) by irradiation of photon energy, with positive ions and electrons generated on its local surface, which might offer an analogous and potential pathway for CO_2 activation. However, Au was inactive in the DRM reaction in thermal catalysis,[9] and cannot be used as the active component of a catalyst for DRM. On the contrary, group-VIII metals were effective in DRM,[10] whereas the effects of photons on the excitation of molecules cannot be well-distinguished since the photon energy would be finally transformed into thermal energy through the decay of hot electrons of the group-VIII metals.[3a] Herein, Au was selected as the plasmonic promoter of the desired catalyst to photocatalytically activate CO_2, and Rh and SBA-15 were employed as the active component and

---

[*] Dr. H. Liu, X. Meng, Dr. T. D. Dao, Dr. H. Zhang, Dr. P. Li, Dr. K. Chang, Dr. T. Wang, M. Li, Dr. T. Nagao, Prof. J. Ye
International Center for Materials Nanoarchitectonics (WPI-MANA)
National Institute for Materials Science (NIMS)
1-1 Namiki, Tsukuba, Ibaraki 305-0044 (Japan)
E-mail: Jinhua.YE@nims.go.jp

Dr. P. Li, Prof. J. Ye
Environmental Remediation Materials Unit
National Institute for Materials Science (NIMS)
1-1 Namiki, Tsukuba, Ibaraki 305-0044 (Japan)

X. Meng, M. Li, Prof. J. Ye
Graduate School of Chemical Science and Engineering
Hokkaido University, Sapporo 060-0814 (Japan)

Prof. J. Ye
TU-NIMS Joint Research Center
School of Materials Science and Engineering
Tianjin University
92 Weijin Road, Nankai District, Tianjin 300072 (China)

Dr. T. D. Dao, Dr. T. Nagao
CREST (Japan) Science and Technology Agency (JST)
4-1-8 Honcho, Kawaguchi, Saitama 332-0012 (Japan)

Prof. J. Ye
Collaborative Innovation Center of Chemical Science and Engineering(Tianjin), Tianjin 300072 (China)

Supporting information for this article is available on the WWW under http://dx.doi.org/10.1002/anie.201504933.

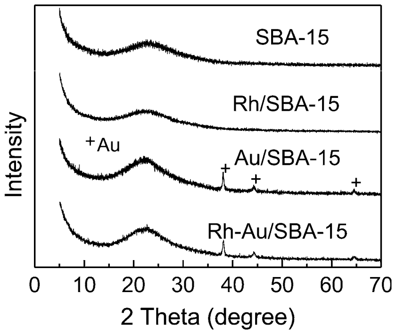

Figure 1. XRD patterns of SBA-15 and the supported fresh catalysts.

Table 1: Elemental analysis and specific surface areas of the catalysts.

Samples	Rh [wt%][a]	Au [wt%][a]	S_{BET} [m^2 g^{-1}][b]
SBA-15	–	–	815
Rh/SBA-15	1.10	–	501
Au/SBA-15	–	0.80	322
Rh-Au/SBA-15	1.50	0.72	375

[a] Analyzed by the ICP-OES method. [b] Obtained by the N_2 adsorption–desorption method through the Brunauer–Emmett–Teller (BET) equation.

support, respectively, because CO_2 activation was the rate-determining step in DRM over Rh/SiO_2.[11]

The crystalline structures of the catalysts were characterized by XRD (Figure 1). The broad peak at about 20–30° was assigned to the amorphous SiO_2, and the sharp and strong peaks centered at 38.0°, 43.7°, and 64.4° were attributed to the Au particles of large sizes. No peaks of Rh could be observed owing to the small sizes and low loadings (the existence of Rh could be detected through XPS in Figure S1 in the Supporting Information and ICP-OES in Table 1; it is about 1.0 wt%). TEM images in Figure S2 indicated the Au and Rh particles were located mainly on the outside surface of SBA-15. The specific surface areas of the catalysts were obtained by the N_2 adsorption–desorption isotherm method (Figure S3) and calculated through Brunauer–Emmett–Teller (BET) equation, and in the range of 300–500 m^2 g^{-1} (Table 1).

The catalytic performances of the catalysts were evaluated in DRM (Figure 2 and Figure S4). Clearly, without irradiation of visible light, the Au/SBA-15 catalyst exhibited almost no activity in DRM (CH_4 conversion 16 μmol g^{-1} s^{-1}, CO_2 conversion 25 μmol g^{-1} s^{-1}), while Rh/SBA-15 and Rh-Au/SBA-15 showed high and similar catalytic activities (CH_4 conversion 1600–1900 μmol g^{-1} s^{-1}, CO_2 conversion 2100–2200 μmol g^{-1} s^{-1}). The results were consistent with the earlier report that Au as promoter was inactive in improving the catalytic performance of a catalyst in the reaction of DRM.[9] On the contrary, it is surprising to discover that, under visible-light irradiation, the catalytic activity over Rh-Au/SBA-15 was much higher than the sum of those over Rh/SBA-15 and Au/SBA-15 (the dotted lines in Figure 2). The detailed reasons for the enhanced performance of Rh-Au/SBA-15 under light illumination will be discussed in the section of mechanism study. For all cases, the conversions of CO_2 were always higher than those of CH_4 owing to the coexistence of reverse water gas shift-reaction as side reaction. Meanwhile, the selectivities to CO and H_2, and the mass balances were nearly 100%, and then the yields to CO and H_2 exhibited analogous trends with the conversions of CO_2 and CH_4. Under visible-light irradiation the performance of Rh/SBA-15 remained constant with the variation of light intensity, owing to the total transformation of photon energy to thermal energy through Rh hot electrons. The total energy input ensured the stable reaction temperature (500 °C).[3a] For Au/SBA-15 and Rh-Au/SBA-15 catalysts, enhanced performances were observed under irradiation of visible light (Figure 2 and Figure S4), and this phenomenon could also be obtained over other Rh-Au/SBA-15 catalysts with Au loadings in the range of 0.47–4.00 wt%. (The successful synthesis of the catalysts were confirmed by the XRD patterns in Figure S5, N_2 adsorption-desorption isotherms in Figure S6 and UV/Vis spectra in Figure S7. The actual Au loadings were analyzed through ICP-OES and shown in Table S1, and their catalytic performances were displayed in Figure S8.) Then it could be speculated that except for the steady reaction temperature (500 °C), Au LSPRs induced by visible light might facilitate the activation of CO_2 and CH_4.

In order to confirm the activation function of LSPRs, the influence of the light wavelength on the performance in DRM reaction was investigated over Rh-Au/SBA-15 catalyst, with several types of filters employed to obtain the desired wavelength range (Figure 3 a). By irradiating light of a wavelength in the range of 490–550 nm, a spherical Au LSPR was

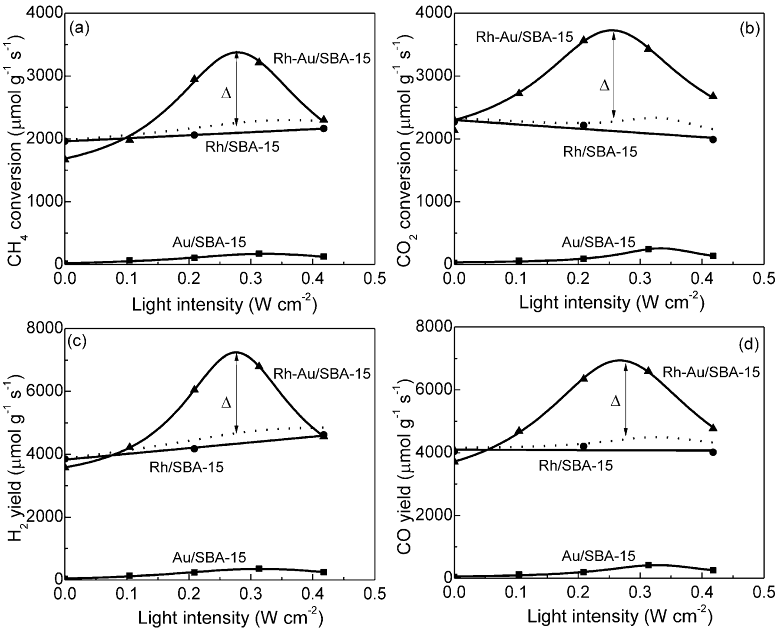

Figure 2. Effects of visible-light intensities on the performance of the catalysts in DRM reaction (The dotted lines are the sum performance of Rh/SBA-15 and Au/SBA-15). a) CH_4 conversion, b) CO_2 conversion, c) H_2 yield, and d) CO yield. Reaction conditions: 500 °C, $CH_4/CO_2 = 1$, flowrate 20.0 mL min^{-1}, 0.0050 g catalyst.

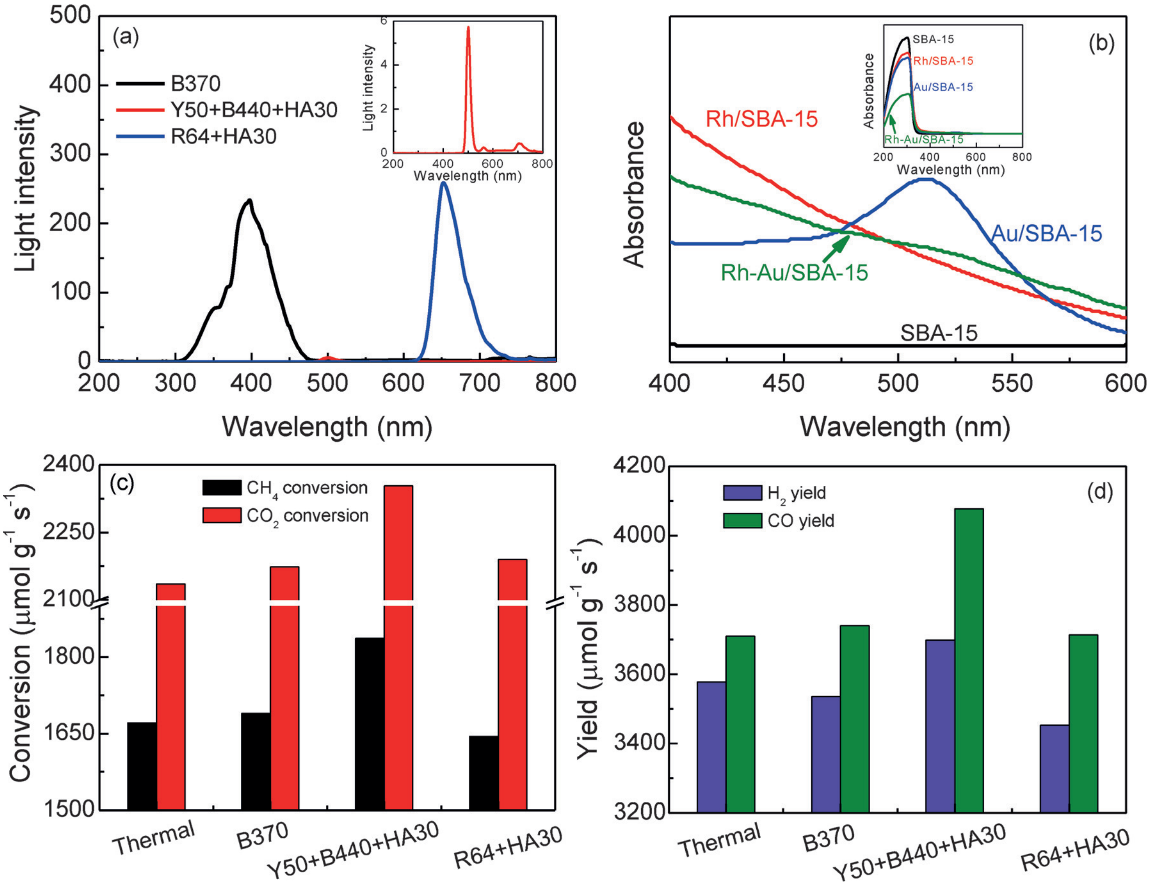

Figure 3. a) Wavelength range obtained with different filter sets (the wavelength of Y50 + B440 + HA30 was shown in the inset), b) UV/Vis spectra of the catalysts (the spectra of 200–800 nm was in the inset), c) CH_4 and CO_2 conversions, and d) H_2 and CO yields without or with light irradiation of different wavelength ranges. Reaction conditions: 500 °C, $CH_4/CO_2 = 1$, flowrate 20.0 mL min^{-1}, 0.0050 g catalyst.

excited (Figure 3b) and an enhanced catalytic activity was observed (CH_4 and CO_2 conversions were 1850 and 2350 μmol g^{-1}s^{-1}, H_2 and CO yields were 3700 and 4050 μmol g^{-1}s^{-1}, in Figure 3c,d), while the performances under light irradiation with wavelengths outside of the Au LSPR band (<480 nm or > 620 nm) were comparable with that without light irradiation (CH_4 and CO_2 conversions were in the ranges of 1650–1750 and 2150–2200 μmol g^{-1}s^{-1}, H_2 and CO yields were in the ranges of 3450–3550 and 3700–3750 μmol g^{-1}s^{-1}, in Figure 3c,d). Additionally, the light intensity adopted to excite Au LSPRs was quite low (160 μW cm^{-2}, in Figure 3a), about one hundredth of the other two cases (they were 17300 and 12050 μW cm^{-2}, respectively, in Figure 3a). Then it could be speculated that it was the Au plasmonic effects that promoted the catalytic performances of Au-containing catalysts in DRM.

For Au-based catalysts under irradiation of visible light, Au LSPR could be triggered and positive ions and electrons could be generated on its local surface,[12] which could be considered as a kind of plasma. The movement of the generated positive ions and electrons could induce an electromagnetic field, with its intensity serving as an indicator of the density of the energetic electrons. In order to study Au LSPR, the electromagnetic simulations were performed using the finite-difference time-domain (FDTD) method (FullWAVE. RSoft, and the model used for the simulation was displayed in Figure S9). Figure 4 reveals the electric field distribution of the catalyst under visible-light excitation of 530 nm. Obviously, with the irradiation of 530 nm single wavelength light, the field intensity ($|E|^2$) was quite weak on Rh/SBA-15 (Figure 4a), since the plasmon resonance of Rh nanoparticles occurred in the UV region,[13] and it was high on Au/SBA-15 (Figure 4b) due to its plasmon resonance in the visible-light region (Figure 3b). Because of the near field coupling between the Rh and Au nanoparticles,[12a] the magnetic field on Rh-Au/SBA-15 (Figure 4c) was four times enhanced compared with Rh/SBA-15, and 1.5 times of that on Au/SBA-15. It should be noted that the field enhancement on Au/SBA-15 was strongest at the centered gaps between Au nanoparticles, which was more than 10 nm away from the SBA-15 surface, while the strongest hot spots on Rh-Au/SBA-15 were located at the Au-Rh and Rh-Rh gaps. Under irradiation of visible light at the LSPR band of Au (530 nm), the hot electrons in Au particles have the tendency to escape from its Fermi level to the surfaces with an energy of 1.8 eV, and the free electrons move more randomly and violently due to thermal excitation and become more energetic at the elevated temperature (500 °C).[14] Considering the properties of plasma and Au LSPR, it could be speculated that CO_2 and CH_4 could be partially polarized by the plasmonic nano-

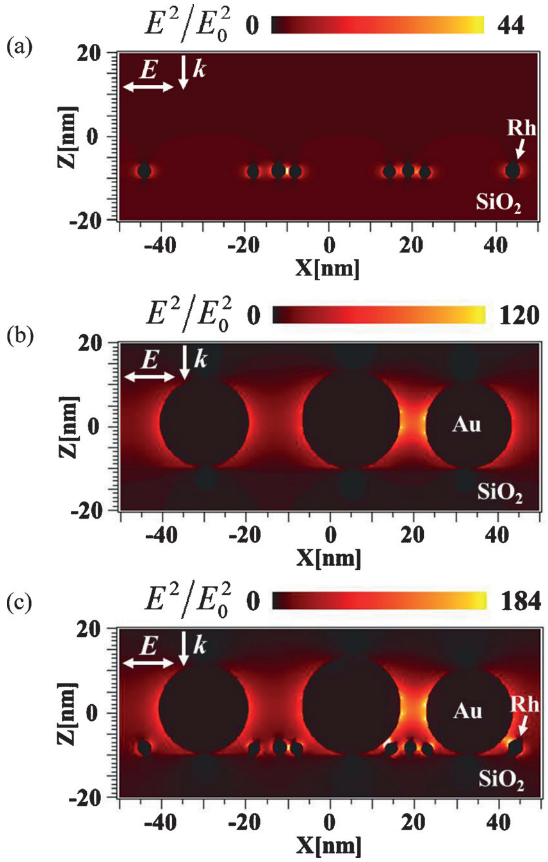

Figure 4. Cross-sectional views of the electromagnetic field distribution and enhancement simulated with FDTD method (The color scale bar shows the electric field enhancement). a) Rh/SBA-15, b) Au/SBA-15, and c) Rh-Au/SBA-15.

metals[15] and electronically excited by the highly energetic plasmon-induced hot electrons by collisional processes[16] [steps (1) and (2), shown below, in Eqs. (1) and (2)].

$$e\,(\text{with high energy}) + CO_2 \rightarrow CO + O + e \tag{1}$$

$$e\,(\text{with high energy}) + CH_4 \rightarrow CH_x + (4-x)H + e \tag{2}$$

Therefore, the catalytic activities of Au/SBA-15 and Rh-Au/SBA-15 increased with light intensity in the range of 0–0.22 W cm^{-2} (Figure 2). However, excessive light irradiation was not favorable for the reaction and the performance deteriorated with the light intensity further increased to 0.44 W cm^{-2} (Figure 2). The Tammann temperature of Au particles is 395 °C,[17] namely, at temperatures higher than 395 °C, the Au particles begin to melt and aggregate. It was reported that the local temperature of the Au particle surface would increase under irradiation of visible light,[18] and the higher intensity of visible light, the higher temperature of the Au particles. Therefore, with the further increase of the visible-light intensity to 0.44 W cm^{-2}, the local temperature of Au particles increased and the mobility of Au particles was enhanced, which resulted in the transformation of Au plasmon energy to its melt energy[15a] and ultimately decreased the catalytic performance. (The TEM images of Rh-Au/SBA-15 catalysts before and after DRM reaction evaluation were available in Figure S2.)

As mentioned above, from Figure 2 it could be observed that the catalytic activity over Rh-Au/SBA-15 was much higher than the sum of those over Rh/SBA-15 and Au/SBA-15 under visible-light irradiation, which was proposed to be related with the different reaction mechanisms.

For all the three catalysts except Au/SBA-15, which exhibited no activity in DRM without light irradiation, the thermal catalytic mechanism was widely studied[4,5] and CH$_4$ and CO$_2$ were regarded to be activated on the Rh active sites through the steps (3) and (4) [Eqs. (3) and (4)], with products H$_2$, CO, and water produced by steps (5)–(9) given in Equations (5) to (9). * and *' are used to denote the active sites on a catalyst for the activation of CH$_4$ and CO$_2$, respectively.

$$CH_4 + {}^* \rightleftharpoons CH_3^* + H \rightleftharpoons CH_2^* + 2\,H \rightleftharpoons CH^* + 3\,H \rightleftharpoons C^* + 4\,H \tag{3}$$

$$CO_2 + {}^{*\prime} \rightleftharpoons CO + O^{*\prime} \tag{4}$$

$$H + H \rightleftharpoons H_2 \tag{5}$$

$$CH_x^* + O^{*\prime} \rightleftharpoons CO + 0.5x\,H_2 + {}^* + {}^{*\prime} \tag{6}$$

$$C^* + CO_2 \rightleftharpoons 2\,CO + {}^* \tag{7}$$

$$CH_x^* + O^{*\prime} \rightleftharpoons CH_{x-1}^* + HO^{*\prime} \tag{8}$$

$$HO^{*\prime} + H \rightleftharpoons H_2O + {}^{*\prime} \tag{9}$$

For the Rh/SBA-15 catalyst, since the LSPR spectrum of Rh nanoparticles heavily tails from the UV region to the visible-light region,[13] LSPR of Au nanoparticles and Rh nanoparticles could couple each other effectively in the visible-light region. As the Rh LSPR was heavily lossy in the visible-light region, the plasmonic energy of Rh nanoparticles would be readily transformed to thermal energy through the damping process of the electron oscillation.[3a] However, the thermal energy generated could not significantly influence the reactor temperature as it was controlled as 500 °C. Therefore, even under irradiation of visible light, the reaction was proposed to be proceeded by the thermally activated methods, steps (3) to (9). However, CO$_2$ activation was the rate-determining step over the Rh/SBA-15 catalyst,[11] which restricted the reaction rate at a limited level. Addition of Au promoter did not improve the catalytic performance in DRM in the thermal catalytic process, whereas the catalytic activity was much improved under irradiation of visible light (Figure 2). Considering the fact that CO$_2$ could be activated by the highly energetic plasmon electrons, then it suggested that in addition to steps (3)–(9), step (1) also existed over the Rh-Au/SBA-15 catalyst under light irradiation, which resulted in promoted CO$_2$ conversions. The promoted CO$_2$ activation further facilitated the Boudouard reaction, which increased the exposed Rh surface by the removal of deposited carbon. (Deposited carbon was analyzed by thermogravimetric analysis, TGA, in Table S2 and Raman method in Figure S10) or active C* species (step 7) and finally provided more active sites for CH$_4$ activation. CH$_4$ could also be faintly activated by plasmon electrons via step (2) (Figure S11).

As for Au/SBA-15 catalyst, it could be seen from Figure 2 that, it exhibited nearly no activity without light irradiation, since the cleavage of CH_4 was requisite to initiate the reaction,[4,5] whereas Au has no ability to break the C–H bond in CH_4.[9] Additionally, both the conversions of CO_2 and CH_4 limitedly increased with the increase of light intensity from 0.0 to 0.22 $\mathrm{W\,cm^{-2}}$. Then it could be predicted that CH_4 cleavage was the limiting step for the DRM reaction over the Au/SBA-15 catalyst. Under light irradiation, CO_2 and CH_4 were electronically excited by the highly energetic plasmon electrons through steps (1) and (2), but not so effective owing to that the energy required to activate CH_4 was quite high and much higher than that for CO_2 activation[16] (The simulated electromagnetic field in Figure 4b implied that there were fewer energetic electrons on Au/SBA-15 catalyst).

In summary, visible-light-induced Au local surface plasmon resonances were firstly reported to possess the ability to activate the nonpolar molecules CO_2 and CH_4, with DRM as the probe reaction. Under visible-light irradiation, Au as promoter could effectively enhance the catalytic performance of Rh/SBA-15 in DRM, since except for the traditional thermal activation method, CO_2 and CH_4 could also be effectively activated by the highly energetic electrons plasmonically excited by Au LSPRs. The distinctive activation method was forecasted to be sufficiently elastic to excite other nonpolar molecules.

Acknowledgements

This work received financial support from the World Premier International Research Center Initiative (WPI Initiative) on Materials Nano-architectonics (MANA), MEXT (Japan), the National Basic Research Program of China (973 Program, grant number 2014CB239301) and the Mitsubishi Foundation.

Keywords: carbon dioxide activation · gold · photocatalysis · surface plasmon resonances · sustainable chemistry

How to cite: *Angew. Chem. Int. Ed.* **2015**, *54*, 11545–11549
Angew. Chem. **2015**, *127*, 11707–11711

---

[1] a) W. Wang, S. Wang, X. Ma, J. Gong, *Chem. Soc. Rev.* **2011**, *40*, 3703–3727; b) M. Mikkelsen, M. Jorgensen, F. C. Krebs, *Energy Environ. Sci.* **2010**, *3*, 43–81; c) D. J. Darensbourg, *Inorg. Chem.* **2010**, *49*, 10765–10780.

[2] a) Z. Zou, J. Ye, K. Sayama, H. Arakawa, *Nature* **2001**, *414*, 625–627; b) A. J. Bard, M. A. Fox, *Acc. Chem. Res.* **1995**, *28*, 141–145; c) H. Tong, S. Ouyang, Y. Bi, N. Umezawa, M. Oshikiri, J. Ye, *Adv. Mater.* **2012**, *24*, 229–251.

[3] a) X. Meng, T. Wang, L. Liu, S. Ouyang, P. Li, H. Hu, T. Kako, H. Iwai, A. Tanaka, J. Ye, *Angew. Chem. Int. Ed.* **2014**, *53*, 11478–11482; *Angew. Chem.* **2014**, *126*, 11662–11666; b) G. Xi, S. Ouyang, P. Li, J. Ye, Q. Ma, N. Su, H. Bai, C. Wang, *Angew. Chem. Int. Ed.* **2012**, *51*, 2395–2399; *Angew. Chem.* **2012**, *124*, 2445–2449.

[4] a) J. B. Claridge, A. P. E. York, A. J. Brungs, C. Marquez-Alvarez, J. Sloan, S. C. Tsang, M. L. H. Green, *J. Catal.* **1998**, *180*, 85–100; b) S. M. Stagg-Williams, F. B. Noronha, G. Fendley, D. E. Resasco, *J. Catal.* **2000**, *194*, 240–249.

[5] a) M. García-Diéguez, I. S. Pieta, M. C. Herrera, M. A. Larrubia, L. J. Alemany, *J. Catal.* **2010**, *270*, 136–145; b) J. Ni, L. Chen, J. Lin, S. Kawi, *Nano Energy* **2012**, *1*, 674–686.

[6] D. Pakhare, J. Spivey, *Chem. Soc. Rev.* **2014**, *43*, 7813–7837.

[7] a) A. J. Morris, G. J. Meyer, E. Fujita, *Acc. Chem. Res.* **2009**, *42*, 1983–1994; b) R. Angamuthu, P. Byers, M. Lutz, A. L. Spek, E. Bouwman, *Science* **2010**, *327*, 313–315.

[8] a) M. Kraus, B. Eliasson, U. Kogelschatz, A. Wokaun, *Phys. Chem. Chem. Phys.* **2001**, *3*, 294–300; b) M. Li, G. Xu, Y. Tian, L. Chen, H. Fu, *J. Phys. Chem. A* **2004**, *108*, 1687–1693.

[9] I. P. Silverwood, N. G. Hamilton, A. R. McFarlane, J. Kapitan, L. Hecht, E. L. Norris, R. M. Ormerod, C. D. Frost, S. F. Parker, D. Lennon, *Phys. Chem. Chem. Phys.* **2012**, *14*, 15214–15225.

[10] P. Ferreira-Aparicio, I. Rodrıguez-Ramos, J. A. Anderson, A. Guerrero-Ruiz, *Appl. Catal. A* **2000**, *202*, 183–196.

[11] J. Nakamura, K. Aikawa, K. Sate, T. Uchijima, *Catal. Lett.* **1994**, *25*, 265–270.

[12] a) S. K. Ghosh, T. Pal, *Chem. Rev.* **2007**, *107*, 4797–4862; b) M. D. Malinsky, K. L. Kelly, G. C. Schatz, R. P. V. Duyne, *J. Am. Chem. Soc.* **2001**, *123*, 1471–1482.

[13] A. M. Watson, X. Zhang, R. A. Osa, J. M. Sanz, F. Gonzalez, F. Moreno, G. Finkelstein, J. Liu, H. O. Everitt, *Nano Lett.* **2015**, *15*, 1095–1100.

[14] C. Starkey, *Therapeutic modalities*, *4th ed.*, F. A. Davis Company, Pennsylvania, **2013**, p. 235.

[15] a) X. Zhang, Y. L. Chen, R. Liu, D. P. Tsai, *Rep. Prog. Phys.* **2013**, *76*, 046401; b) S. Sun, W. Wang, L. Zhang, M. Shang, L. Wang, *Catal. Commun.* **2009**, *11*, 290–293.

[16] a) C. Liu, R. Mallinson, L. Lobban, *J. Catal.* **1998**, *179*, 326–334; b) A. Oumghar, J. C. Legrand, A. M. Diamy, N. Turillon, *Plasma Chem. Plasma Process.* **1995**, *15*, 87–107; c) C. Liu, G. Xu, T. Wang, *Fuel Process. Technol.* **1999**, *58*, 119–134.

[17] G. M. Veith, A. R. Lupini, S. Rashkeev, S. J. Pennycook, D. R. Mullins, V. Schwartz, C. A. Bridges, N. J. Dudney, *J. Catal.* **2009**, *262*, 92–101.

[18] F. Wang, C. Li, H. Chen, R. Jiang, L. Sun, Q. Li, J. Wang, J. C. Yu, C. Yan, *J. Am. Chem. Soc.* **2013**, *135*, 5588–5601.

Received: June 1, 2015